7. K. Cherchin'yani, Theory and Application of the Boltzmann Equation [Russian translation], Mir, Moscow (1978).
8. G. Batchelor and G. Green, "Hydrodynamic interaction of two small freely moving spheres in a linear flow field," [Russian translation], Mekhanika, No. 22 (1980).
9. Yu. L. Klimontovich, Statistical Physics [in Russian], Nauka, Moscow (1982).
10. L. D. Landau and E. M. Lifshits, Theoretical Physics [in Russian], Vol. 10, Nauka, Moscow (1979).
11. V. V. Struminskii, "On a method of solving a system of kinetic equations for gas mixtures," Dokl. Akad. Nauk SSSR, 237, No. 3 (1977).
12. B. V. Alekseev, Mathematical Kinetics of Reacting Gases [in Russian], Nauka, Moscow (1982).
13. R. G. Barantsev, Rarefied Gas Interaction with Streamlined Surfaces [in Russian], Nauka, Moscow (1975).
14. H. Mott-Smith, "Solution of the Boltzmann equations for a shock," Mekhanika [Russian translation], 17, No. 1 (1953).
15. H. W. Liepmann, K. Narasiwha, and M. T. Chahine, "Structure of a plane shock layer," Phys. Fluids, 5, No. 11 (1962).
16. G. G. Tivanov, "On certain exact solutions of a kinetic equation of Boltzmann type," Izv. Vyssh. Uchebn. Zaved. Fiz., No. 4 (1984). (Dep. in VINITI, No. 1567-84).
17. B. Schmidt, "Electron beam density measurements in shock waves in argon," J. Fluid Mech., 39, No. 2 (1969).
18. M. N. Kogan, Dynamics of a Rarefied Gas [in Russian], Nauka, Moscow (1967).

DYNAMICS OF DROPLET BREAKUP IN SHOCK WAVES

V. M. Boiko, A. N. Papyrin, and S. V. Poplavskii

UDC 532.529.5/6

Study of the principles of acceleration and fragmentation of droplets during interaction with a high speed gas flow is of interest because of its important practical applications (for example, atomization of liquids in various technological processes, energy generation equipment, detonation wave propagation in gas–droplet systems, etc.). In particular, the problem of heterogeneous detonation in a gas–droplet system requires detailed study of the processes of acceleration, deformation, fragmentation, ignition, and combustion of droplets within shock waves at Mach numbers M = 2-6 for Weber numbers $We = \rho u^2 d_0 \sigma^{-1} > 10^3$ and Reynolds numbers $Re = \rho u d_0 \mu^{-1} > 10^3$. Here ρ, u, μ are the density, velocity and viscosity of the gas, d_0 is the initial droplet diameter, and σ is the liquid surface tension.

Numerous studies of droplet interaction with shock waves are reflected in reviews [1-3], which considered characteristic regimes of droplet breakup and indicated corresponding parameter ranges. Thus, according to [2], for $We > 10^3$, $Re > 10^3$, corresponding to the explosive droplet decay range, the following pattern exists. Over a time interval $0 < t < t_0$ (where $t_0 = d_0 \rho_\ell^{0.5} (\rho u^2)^{-0.5}$, ρ_ℓ being the liquid density) a droplet collapses into a disk of size $d \sim 3d_0$. At time $t \sim (0.1\text{-}0.5)t_0$ a thin layer of liquid begins to break away from the equatorial region of the deformed drop and then breaks into pieces. The dimensions of the microparticles thus formed are in the range d ~ 1-10 μm [4, 5]. Due to instability of the phase separation boundary at $t \simeq t_0$ explosive decay of the disk begins, reaching its greatest velocity at $t \sim (1.5\text{-}2)t_0$ and ending at $t \sim (4\text{-}5)t_0$. The dimensions of the particles formed by this explosive decay are of the order of the thickness of the disk into which the droplet was deformed at the time of maximum deformation $d \sim (0.1\text{-}0.2)d_0$ [1]. The nucleus of the disintegrating drop moves along a trajectory $x d_0^{-1} \sim (0.5\text{-}1.4) t^2 t_0^{-2}$ [6]. However, despite the large number of experiments which have been performed, many questions concerning droplet breakup in shock waves remain little studied. Among these, in particular, are the effect of viscosity on droplet destruction dynamics, the size of the microparticles formed, the process of evaporation of the disintegrating droplet, etc.

Novosibirsk. Translated from Zhurnal Prikladnoi Mekhaniki i Tekhnicheskoi Fiziki, No. 2, pp. 108-115, March-April, 1987. Original article submitted January 16, 1986.

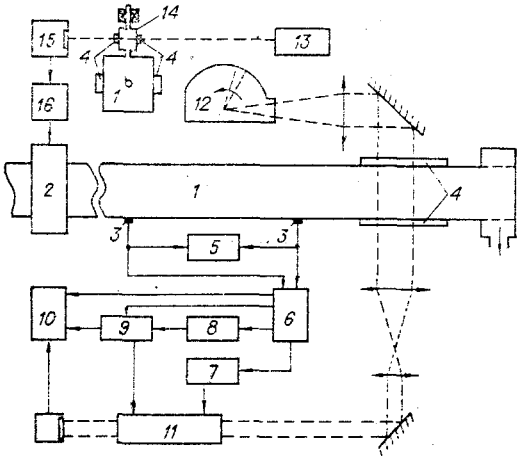

Fig. 1

It should be noted that practically all the major results published previously were obtained either with SFR type optomechanical cameras [5, 7] or by frame-by-frame photography [1, 4, 8] where only a single exposure is made in one device operating cycle. The first of these techniques does not produce sufficient time–space resolution, while with the second, uncertainty connected with scattering of experimental parameters upon transition from one "shot" to the next can be significant.

This study will offer results of a study of the processes of acceleration, deformation, destruction, and evaporation of droplets of various liquids in the flow behind a shock wave at M = 2-4, obtained by multiple-frame laser photography, which provided continuous recording of droplet behavior during a single "shot" with time resolution of ~10^{-8} sec.

1. Experimental Apparatus. Liquid droplet interaction with a shock wave was studied with experimental apparatus diagrammed in Fig. 1. Its major components are: a shock tube with low pressure chamber (LPC) 1 and high pressure chamber (HPC), separated by an electromagnetically controlled valve 2, diagnostic apparatus, and control and synchronization circuits. The LPC has a working section of 56 × 56 cm, 1.7 m long, provided with piezoelectric sensors 3 and 20 × 200 mm windows 4 for performing optical measurements. The droplet generator 14 was located on the upper wall of the low pressure chamber and had a trigger device allowing release of one or several droplets at the required time. The droplet size was controlled by the diameter of the capillary through which liquid was supplied. Experiments were performed with water, alcohol, glycerine, and tridecane with dimensions from 0.5 to 3.5 mm. The initial gas pressure in the channel p_0 = 20-100 kPa, with initial gas temperature T_0 = 290 K. Helium at a pressure of 1-5 MPa was used as the driver gas. Measurement of shock wave velocity and synchronization of the diagnostic apparatus were performed by piezoelectric pressure sensors and an electronic chronometer 5. Gas parameters behind the shock wave front were calculated from known relationships for shock tubes [9].

The dynamics of droplet behavior in the shock wave were studied by high speed multiframe shadow photography. Exposure duration, the number of frames, and frame frequency were controlled by the light source 11 while spatial separation of frames was done by a ZhFR-3 camera 12. The light source used was a ruby laser, operating in the stroboscopic mode [10], thus producing series of from 1 to 50 light pulses ~$3 \cdot 10^{-8}$ sec in duration with the interval between pulses lying in the range Δt = 10-100 μsec to an accuracy of 0.2 μsec. Spatial resolution of the optical system referenced to the object plane comprised ~30 lines/mm, with frame size of 18 × 24 mm.

The synchronization system provided the necessary sequencing in time for triggering the elements of the shock tube and diagnostic equipment. After the triggering device operates, on its way to the axis of the shock tube the droplet intersects the beam from a helium–neon laser 13 used for synchronization, whereupon the signal from photodiode 15 is applied to the delayed pulse generator 16, which after the necessary time delay (~10^{-2} sec) sends a pulse to the valve control circuitry. Operation of the laser stroboscopic light source was controlled by sync pulse generator 6, which is triggered by signals from the piezoelectric sensors. Control pulses with the required time delays are fed from the output of this generator to the pump lamp ignition circuit 7, the trigger input of oscilloscope 10, high voltage pulse

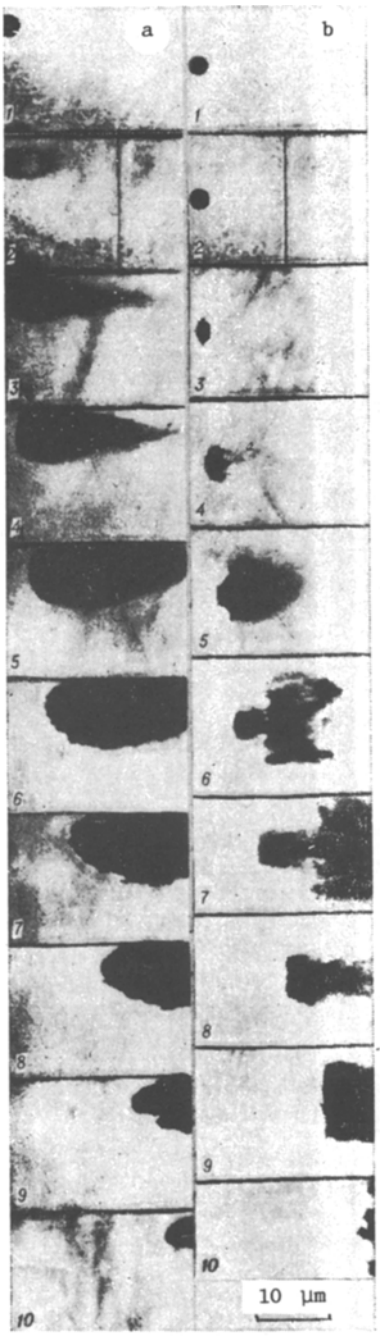

Fig. 2

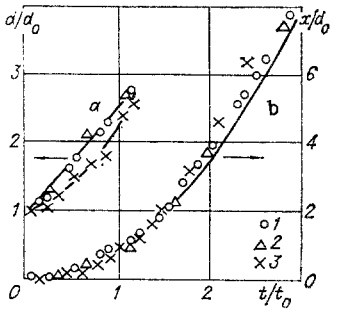

Fig. 3

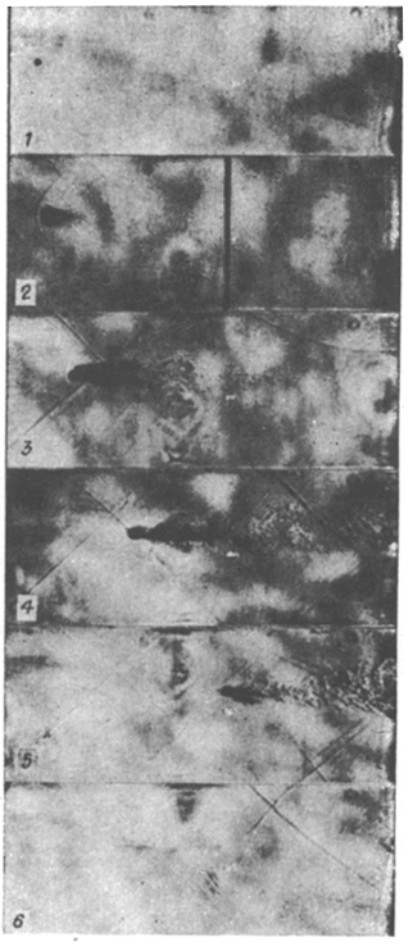

Fig. 4

shaper 9, and timing generator 8, which latter provides the necessary time relationship between light pulse generation and passage of the shock wave front through the region to be studied.

2. Experimental Results. We will examine the experimental data obtained for interaction of droplets of various liquids with a shock wave at M = 2-4.

Figure 2a shows a series of shadow photographs of a water droplet with d_0 = 3.2 mm disintegrating in a gas flow behind a shock wave (M = 2.37, $p_0 = 10^5$ Pa, We = $5.3 \cdot 10^4$, Re = $2.3 \cdot 10^5$, Δt = 30 μsec). Frame 1 shows an image of the droplet before interaction with the shock wave. In frame 2 ($t \simeq 20$ μsec) the shock wave front propagating from left to right is visible together with the compression discontinuity exiting onto the droplet (interaction time is reckoned from the moment of contact of the wave front with the frontal surface of the droplet). By this time deformation of the droplet core is noticeable and a cloud of microparticles torn from the surface is formed. With increase in the interaction time (frames 3-6) the transverse diameter of the deformed core increases together with the dimensions of the microparticle

cloud, the form of which corresponds to the gas flow accompanying flow over a blunt body. From the measured length of the wake x_i and its distance from the shock wave front x_s one can estimate the induction period for breakup of the microparticle t_i (distance is also measured from the forward surface of the droplet).

The experiments showed that the velocity of the far boundary of the microparticle cloud coincides with the gas velocity as calculated with the known relationships of [9]. Then, assuming that u = const in the vicinity of the droplet, we obtain $t_i = x_s V^{-1} - x_i u^{-1}$, where V is the velocity of the shock wave front. For the given experiment t_i = 6.8 μsec.

Maximum deformation of the droplet core $d \sim 2.8\, d_0$ is reached in $t \approx 110$ μsec $\approx 1.2\, t_0$ (frame 5). Because of the accelerated motion of the droplet wavelike perturbations are generated on its forward surface, which become noticeable at $t \approx 80$ μsec $\approx 0.9\, t_0$ (frame 4) and is well manifested at t = 140 μsec = 1.5 t_0 (frame 6). The wavelength of these perturbations $\lambda \approx 1.2$ mm. At the same time (t = 140 μsec = 1.5 t_0) the breakoff of secondary relatively coarse (~1 mm) droplets from the periphery of the deformed core, which droplets in turn then disintegrate by breakoff of a surface layer of liquid (frames 5-10). The visible transverse dimension of the droplet core decreases and its central region disintegrates. The time required for complete destruction of the droplet is $t \approx 320$ μsec $\approx 3.5\, t_0$. A similar pattern occurred in all the experiments which studied the behavior of droplets of different liquids ($\rho_\ell \sim 0.7$-1.5 g/cm^3, $\mu_\ell \sim 10^{-3}$ Nsec/m^2, $\sigma \sim (2\text{-}7)\cdot 10^{-2}$ n/m) in a shock wave at M = 2-4, which agrees well with the results of [1, 4, 5, 7, 8]. The experiments showed that the induction time for breakaway of liquid from the droplet surface is independent of its initial size at d_0 = 0.5-3.5 mm.

Figure 2b shows a series of shadow photographs illustrating breakup of a droplet of glycering with d_0 = 2.6 mm (frame 1) under experimental conditions close to those of Fig. 2a (M = 2.37, $p_0 = 10^5$ Pa, We = $4.9\cdot 10^4$, Re = $1.9\cdot 10^5$, Δt = 30 μsec). It is evident that with increase in liquid viscosity μ_ℓ by 10^3 times the pattern of droplet disintegration changes greatly. A characteristic feature of shock wave interaction with a glycerine droplet is the nonsimultaneous occurrence of the deformation and destruction processes. Deformation begins with the downwind side of the drop. After t = 15 μsec (frame 2) it is barely noticeable. With passage of time the droplet takes on the form of a truncated cone with base turned toward the incident flow (frame 3). During the deformation process a sharp edge is formed about the periphery of the base, the transverse dimensions of which increase with time as it moves away from the base. The droplet takes on a characteristic "hat" form with flat top (frames 4, 5). The maximum deformation $d \sim 2.9\, d_0$ is reached at $t \approx 105$ μsec $\approx 1.25\, t_0$ (frame 5). The disintegration process begins at $t_i \sim 50$ μsec and takes place by "stripping" from the brim of the "hat" of a liquid film with breakup of the latter near the droplet core (frames 4, 5) and in a later stage by a "parachute and jet" mechanism [3], i.e., due to blowoff of a pocket (the "parachute") from the hat brim with chaotic breakup of this pocket. The "hat" brim is completely destroyed by $t \approx 135$ μsec = 1.6 t_0 (frame 6). The remaining droplet core then disintegrates in a similar manner, its transverse dimensions constantly increasing (frames 7-10). By $t \sim 225$ μsec (frame 9) the droplet core loses its integrity. The remaining droplet takes on a chaotic form and decays completely by $t \approx 345$ μsec $\approx 4.1\, t_0$. This pattern of glycerine droplet disintegration corresponds to the pattern of destruction of droplets of low viscosity liquids (water, kerosene) in a shock wave with M = 1.05-1.15 [1].

Figure 3 presents data on deformation (a) and displacement (b) of the droplet core behind a shock wave (M = 2.37, $p_0 = 10^5$ Pa) for various liquids (1, H_2O; 2, C_2H_6O; 3, $C_3H_8O_3$). The data on deformation of the low viscosity liquids (water, alcohol) can be approximated well by a straight line. Deformation of the glycerine droplet follows a more complex law. However maximum deformation $d \sim (2.8\text{-}2.9)d_0$ is reached by all droplets at practically the same time $t \approx (1.2\text{-}1.3)t_0$. Despite the significant difference in form of the windward sides of low viscosity and superviscous liquids, in the initial stage of acceleration (up to $t \sim 1.5\, t_0$) displacement of their cores occurs along identical trajectories $x/d_0 = 0.85(t/t_0)^2$, which corresponds to a droplet aerodynamic resistance coefficient $C \approx 2.3$.

The results presented indicate that for identical values of We, Re, liquid viscosity has an effect on the character of deformation and disintegration. It has been established that with increase in viscosity by a factor of 10^3 the droplet disintegration induction time increases by ~10 times, while the time at which maximum deformation is reached and the total droplet destruction time remain unchanged.

The experimental technique used also permits observation of the dynamics of evaporation of the disintegrating droplet. Figure 4 illustrates the process of disintegration and

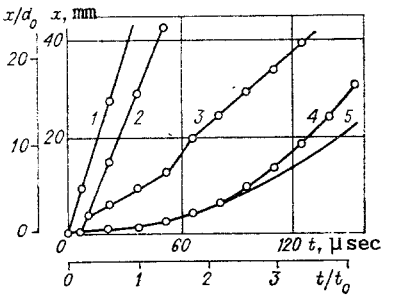

Fig. 5

TABLE 1

Liquid	M	d_0, mm	We·10⁻⁴	Re·10⁻⁵	t_i, μsec		d_1, μm		t_v, μsec
					experiment	calculation, Eq. (3)	experiment	calculation, Eq. (5)	experiment
$C_3H_8O_3$	2.37	2.6	4.9	1.9	50.5	78.0	—	462	—
H_2O	2.37	3.2	5.3	2.3	6.8	6.5	—	4.0	—
C_2H_6O	2.37	2.4	13.4	1.8	6.2	5.3	—	3.2	—
H_2O	2.46	0.7	1.3	0.5	5.0	5.5	4.7	3.6	50
C_2H_6O	2.46	0.7	4.2	0.5	4.3	4.4	4.3	3.0	14
$C_{13}H_{28}$	3.4	0.7	3.0	0.2	6.2	5.9	3.3	4.2	9
$C_{13}H_{28}$	3.8	1.9	12.1	0.6	4.6	4.4	3.0	3.7	5
$C_{13}H_{28}$	3.8	0.9	6.3	0.3	4.6	4.4	3.0	3.7	5

evaporation of a drop of tridecane with $d_0 \sim 0.7$ mm (frame 1) in a shock wave (M = 3.4, p_0 = 28 kPa, Δt = 25 μsec). It is evident that at t = 23 μsec (frame 2) the transverse dimension of the deformed droplet reaches a value of $d \simeq 2.5\, d_0$, and a cloud of torn away microparticles entering the wake of evaporating liquid is clearly visible behind the droplet. The departing main shock wave and the trailing compression discontinuity adjacent to the wake at the point of intense liquid evaporation are clearly visible. With increase in interaction time the extent of the cloud of unevaporated microparticles increases, with the beginning of evaporation already visible on the lateral surface of the cloud (frames 3-5). The droplet disintegrates and is completely evaporated at $t \simeq 110$ μsec $\simeq 4\, t_0$ (frames 5, 6).

Figure 5 shows displacement of the droplet core 4, the boundary between the microparticle cloud and the evaporating liquid 3, the edge of the evaporating liquid wake further from the droplet 2, and the shock wave front 1, obtained in an experiment with a tridecane droplet d_0 = 1.9 mm and a shock wave with M = 3.8, p_0 = 28 kPa. The slope of line 1 corresponds to the shock wave velocity. The rate of displacement of boundary 2 is equal to the gas velocity behind the shock wave front. In the curve of displacement of boundary 3 there is a characteristic cusp corresponding to $t = (1.3\text{-}1.6)t_0$. As was noted earlier, the explosive breakup mechanism begins to act at this time. The experimental data on displacement of the droplet core 4 is in good agreement with the parabolic dependence $x/d_0 = 0.85(t/t_0)^2$ up to the time $t \simeq 2t_0$ (Fig. 5, curve 5), with the divergence increasing at later times. At each moment of time the extent of the cloud of unevaporated microdroplets is determined by the distance between curves 4 and 3, and the length of the wake of completely evaporated liquid wake, by the distance between curves 3 and 2. The point of intersection of line 2 with the time axis defines the induction time for removal of liquid from the droplet surface t_i. The induction time for microparticle evaporation $t_v = t_{32} - t_i$, where t_{32} is the time at which evaporation commences, determined by the intersection of curves 3 and 2. Results of t_i and t_v measurements for the liquids considered above under various conditions are presented in Table 1.

The measured values of t_v can be used to estimate the size of the microparticles torn from the drop surface, d_1. Assuming that the heat exchange conditions with the gas for particles located in the periphery of the cloud are similar to heat exchange conditions for an isolated drop at rest relative to the gas, the time required for heating a microparticle with diameter d_1 to the liquid boiling point T_v can be determined from the expression

$$t_v = \rho_l \frac{d_1^2 c_l}{12h} \ln \frac{T - T_0}{T - T_v}.$$

where c_ℓ is the specific heat of the liquid, h, T are the thermal conductivity and temperature of the gas, m and T_0 is the initial droplet temperature.

Characteristic values of d_1 calculated with this expression are presented in Table 1, and comprise 3-5 μm in the range M = 2-4, We = 10^4-10^5, Re = 10^4-10^5.

3. Evaluation of Results. The studies performed indicate that the major role in disintegration of low viscosity liquids in a shock wave with M = 2-4 is played by the mechanism of removal of a surface layer of liquid, which acts after an induction period t_i and continues through the complete decay of the droplet. This same mechanism determines the size of the removed microparticles d_1. If the criterion Bo = $\rho_\ell a d_0^2 \sigma^{-1} > 5 \cdot 10^3$ [11,12] (where a is the droplet acceleration) then after a time t_λ an explosive breakup mechanism begins to act, due to instability of the accelerating phase separation boundary (Taylor instability). The characteristic time for development of this instability t_λ, defined as the time interval before commencement of breakoff of coarse (~λ) particles, is described well by the expression [11, 12]

$$t_\lambda t_0^{-1} = 20\,\mathrm{Bo}^{-0,25} \simeq 23\,\mathrm{We}^{-0,25}.$$

Destruction of a glycerine droplet also begins with "peeling" of the surface layer of liquid from the equator of the deformed core. In a later stage, as was indicated above, decay is accomplished in a "parachute and jet" form. Waves are absent from the forward surface of the glycerine droplet, apparently because of the damping effect of viscosity.

Up to the present two models have been used to explain droplet breakup by removal of a surface layer of liquid. According to model 1 [5, 13] destruction occurs by "peeling" of the liquid boundary layer from the periphery of the deformed droplet core. The mean dimensions of particles formed by fragmentation of the torn away liquid film is estimated to be the same as the thickness of the liquid boundary layer in the equatorial region of the droplet [13]

$$d_1 = 2{,}4 d_0 (\mu_\ell/\mu)^{0,5} (\rho_\ell/\rho)^{-0.25} \mathrm{Re}^{-0.5}, \tag{1}$$

while the induction time for this process is determined by the boundary layer formation time and comprises [13]

$$t_i = 0{,}37 t_0 = 0{,}37 d_0 u^{-1} (\rho_\ell/\rho)^{0,5}. \tag{2}$$

According to model 2 [14], disintegration takes place by tearing away of microparticles from the peaks of wave perturbations formed on the lateral surface of the droplet, formed as the result of development of Kelvin–Helmholtz instability. The size of these particles is then proportional to the mean wavelength of these perturbations [14]:

$$d_1 = A\lambda_i, \tag{3}$$

where

$$\lambda_i = 9\pi \sqrt[3]{16}\, \mu^{0,66} \sigma^{0,33} \rho_\ell^{-0,33} (\beta \rho u^2)^{-0,66}, \tag{4}$$

and the induction time is given by the expression [15]

$$t_i = B \rho_\ell^{0.33} \sigma^{0,66} \mu_\ell^{0,33} (\beta \rho u^2)^{-1,33}. \tag{5}$$

Here A and B are proportionality coefficients and β is the screening coefficient.

Commencing from this model, we find the conditions for breakoff of the liquid surface layer assuming that the breakoff is realized if upon the windward side of the droplet at least one wave perturbation peak is formed, i.e.,

$$\lambda_i \leqslant \pi d_0/4. \tag{6}$$

Rewriting Eq. (4) in the form

$$\lambda_i = 9\pi \sqrt[3]{16}\, \beta^{-0,66} d_0\, \mathrm{We}^{-0,66}\, \mathrm{Lp}^{-0,33} \tag{7}$$

and substituting Eq. (7) in Eq. (6), we obtain

$$\mathrm{We} \geqslant 864 \beta^{-1} \mathrm{Lp}^{-0,5}, \tag{8}$$

where Lp = $d_0 \rho_\ell \sigma \mu_\ell^{-2}$ is the Laplace number. Since according to [16], β ≃ 0.05, we may write condition (8) as

$$We \geqslant 1.7 \cdot 10^4 Lp^{-0.5}. \quad (9)$$

Based upon this criterion, we can explain the difference in the decay patterns of water and glycerine droplets. Thus, comparison of the scale parameters shows that for the water drop $\lambda_i \ll \pi d_0/4$ and its destruction occurs by the mechanism of model 2. This is also experimentally confirmed by the observed independence of induction time from initial drop diameter, which corresponds to Eq. (5). For a glycerine droplet $\lambda_i > \pi d_0/4$, and its destruction occurs by "peeling" of the liquid boundary layer, as indicated by a characteristic feature in the pattern of glycerine drop disintegration – formation of a sharp edge on its equator (see Fig. 2b, frame 3). The validity of criterion (9) is also confirmed by the experimental data of [1], in which characteristics of disintegration of a kerosene drop Eq. (9) is not satisfied and its decay is similar to the initial stage of glycerine drop decay described above. Satisfactory quantitative agreement of experimental data with values calculated with Eqs. (3), (5) for d_i, t_i exists at A = 0.2, $B = (K/\sigma)^{0.5}$, where K = 500 N/m (see Table 1).

LITERATURE CITED

1. B. E. Gel'fand, S. A. Gubin, and S. M. Kogarko, "Varieties of droplet fractionation in shock waves and their characteristics," Inzh. Fiz. Zh., 27, No. 1 (1974).
2. B. E. Gel'fand, "Current state and problems of studying detonation in liquid drop–gas systems," in: Detonation [in Russian], Chernogolovka (1977).
3. A. I. Ivandaev, A. G. Kutushev, and R. I. Nigmatulin, "Gas dynamics of multiphase media. Shock and detonation waves in gas suspensions," Itogi. Nauki. Tekh., VINITI, Ser. Mekh. Zhidk. Gaza, 1, (1981)
4. O. G. Engel, "Fragmentation of wave drops in the zone behind an air shock," J. Res. Nat. Bur. Stand., 60, No. 3 (1958).
5. A. A. Runger and J. A. Nicholls, "Aerodynamic scattering of liquid drops," AIAA J., 7, No. 2 (1969).
6. G. A. Simons, "Liquid drop acceleration and deformation," AIAA J., 14, No. 2 (1976).
7. B. M. Belen'kii and G. A. Evseev, "Experimental study of droplet destruction under the action of gas moving behind a shock wave," Izv. Akad. Nauk SSSR, Mekh. Zhidk. Gaza, No. 2 (1974).
8. G. D. Waldman, W. G. Reineche, and D. C. Glenn, "Raindrop break-up in the shock layer of a high speed vehicle," AIAA J., 10, No. 9 (1972).
9. Kh. A. Rakhmatullin and S. S. Semenov (eds.), Shock Tubes [Russian translation], IL, Moscow (1962).
10. V. M. Boiko, A. A. Karnaukhov, et al., "Multiexposure photorecording in particles in high speed two-phase flows," Zh. Prikl. Mekh. Tekh. Fiz., No. 3 (1982).
11. E. Y. Hurper, G. W. Brube, and I-Dee Ghang, "On the break-up of accelerating liquid drops," J. Fluid Mech., 52, No. 3 (1972).
12. P. G. Simpkins and E. L. Bales, "Water drop response to sudden acceleration," J. Fluid Mech., 55, No. 4 (1972).
13. A. A. Ranger, "Shock wave propagation through a two-phase medium," Acta Astronaut., 17, No. 4/5 (1972).
14. E. Mayer, "Theory of liquid atomization in high velocity gas streams," ARS J., 31, No. 12 (1961).
15. A. A. Borisov, B. E. Gel'fand, et al., "Intensification of weak shock waves in a hot two-phase gas–liquid system," Zh. Prikl. Mekh. Tekh. Fiz., No. 1 (1970).
16. P. H. Leblond and A. Mysak, Waves in the Ocean, Elsevier (1978).